A Secreted Salivary Inositol Polyphosphate 5-Phosphatase from a Blood-Feeding Insect: Allosteric Activation by Soluble Phosphoinositides and Phosphatidylserine

John F. Andersen* and José M. C. Ribeiro

Laboratory of Malaria and Vector Research, National Institute of Allergy and Infectious Diseases, National Institutes of Health, Bethesda, Maryland 20892

Received November 30, 2005; Revised Manuscript Received March 1, 2006

ABSTRACT: Type II inositol polyphosphate 5-phosphatases (IPPs) act on both soluble inositol phosphate and phosphoinositide substrates. In many cases, these enzymes occur as multidomain proteins in which the IPP domain is linked to lipid-binding or additional catalytic domains. *Rhodnius prolixus* IPPRp exists as an isolated IPP domain which is secreted into the saliva of this blood-feeding insect. It shows selectivity for soluble and lipid substrates having a 1,4,5-trisphosphate substitution pattern while only poorly hydrolyzing substrates containing a D3 phosphate. With soluble *di*C8 PI(4,5)P_2 as a substrate, sigmoidal kinetics were observed, suggesting the presence of allosteric activation sites. Surprisingly, IPPRp-mediated hydrolysis of PI(4,5)P_2 and PI(3,4,5)P_3 was also stimulated up to 100-fold by *di*C8 PI(4)P and *di*C8 phosphatidylserine (PS). The activation kinetics were again sigmoidal, demonstrating that the allosteric sites recognize nonsubstrate phospholipids. Activation was positively cooperative, and analysis by the Hill equation suggests that at least three to four allosteric sites are present. In a vesicular system, hydrolysis of PI(4,5)P_2 followed a surface dilution kinetic model, and as expected, PS was found to be strongly stimulatory. If allosteric activation of type II IPPs by PI(4)P and PS is a widespread feature of the group, it may represent a novel regulatory mechanism for these important enzymes.

Inositol phosphates and phosphoinositides are in involved in many cellular processes related to signal transduction, secretion, and cytoskeletal structure (*1*−*4*). PI(4,5)P_2,[1] as a component of membranes, is involved in cytoskeletal attachment, vesicle secretion, endocytosis, and membrane trafficking, apparently by serving as an anchor for proteins containing phosphoinositide-binding domains, including the pleckstrin homology (PH) domain (*5*). A second phosphoinositide, PI(3,4,5)P_3, is also important as a product of the phosphoinositide 3-kinase pathway, which is involved in many cellular functions (*6*). Like PI(4,5)P_2, it acts by recruiting proteins containing specific binding domains such as PX and FYVE (*5*, *7*). The soluble inositol phosphate Ins(1,4,5)P_3 occurs in the cytoplasm and is a product of hydrolysis of PI(4,5)P_2 by phospholipase C. It is an essential signal transduction mediator regulating calcium mobilization (*8*).

Numerous enzymes are involved in the metabolism of inositol phosphates and phosphoinositides, including kinases, phosphatases, and phospholipases. Inositol polyphosphate 5-phosphatases (IPPs) regulate the pool of 5-phosphorylated inositol phosphates and phosphoinositides, thereby influencing cellular processes that require PI(4,5)P_2, PI(3,4,5)P_3, and Ins(1,4,5)P_3. This enzyme group is divided into four classes known as types I−IV IPPs (*9*). Type I phosphatases are specific for soluble inositol phosphates and are thought to function as terminators of calcium signaling. Type II enzymes attack both soluble inositol phosphate and phosphoinositide substrates and hydrolyze substrates either with or without a phosphate group at the D3 position. The type III group also hydrolyzes both soluble and phospholipid substrates, including PI(4,5)P_2 and PI(3,4,5)P_3 (*10*). Type IV enzymes were originally thought to hydrolyze only PI(3,4,5)P_3 but will accept PI(4,5)P_2 if certain detergents are added to the reaction mixture (*10*).

The crystal structure of a yeast type II IPP domain from SPsynaptojanin, a protein that is similar to vertebrate synaptojanin, has been determined (*11*). The active site of the enzyme binds inositol phosphates or the headgroup of phosphoinositides, placing them in the proximity of a bound metal ion which assists in catalysis. Additional surfaces surrounding the binding site appear to be involved in interaction with membrane interfaces, an idea supported by site-directed mutagenesis studies (*11*). Type II and type III phosphatases often occur as domains in larger proteins containing protein-binding or additional enzymatic domains (*9*, *11*). For example, synaptojanin and SPsynaptojanin contain a Sac1-like domain that also has inositol phosphatase activity, particularly toward monophosphorylated phosphoinositides (*4*).

In this report, we describe a new member of this family, IPPRp, which is secreted into the saliva of the blood-feeding

* To whom correspondence should be addressed: Laboratory of Malaria and Vector Research, NIAID, NIH, Twinbrook 3 Building, 12735 Twinbrook Parkway, Bethesda, MD 20892. Telephone: (301) 435-2967. Fax: (301) 402-2201. E-mail: jandersen@niaid.nih.gov.

[1] Abbreviations: PC, L-phosphatidylcholine; PS, L-phosphatidylserine; Ins(1,4,5)P_3, D-*myo*-inositol 1,4,5-trisphosphate; Ins(1,3,4,5)P_4, D-*myo*-inositol 1,3,4,5-tetrakisphosphate; Ins(1,4)P_2, D-*myo*-inositol 1,4-bisphosphate; Ins(1,2,3,4,5,6)P_6, D-*myo*-inositol 1,2,3,4,5,6-hexakisphosphate; PI(4,5)P_2, D-*myo*-phosphatidylinositol 4,5-bisphosphate; PI(3,4,5)P_3, D-*myo*-phosphatidylinositol 3,4,5-trisphosphate; PI(4)P, D-*myo*-phosphatidylinositol 4-phosphate; PI(5)P, D-*myo*-phosphatidylinositol 5-phosphate; IPP, inositol polyphosphate 5-phosphatase.

10.1021/bi052444j CCC: $33.50
Published on Web 04/06/2006

insect *Rhodnius prolixus*, a vector of the medically important trypanosomatid parasite *Trypanosoma cruzi*, where it apparently acts to facilitate the ingestion of blood. It is unique in being extracellular and does not contain additional protein domains outside of the 5-phosphatase domain. We find that the enzymatic activity is activated in an allosteric manner by the substrate PI(4,5)P_2, the product PI(4)P, and the membrane phospholipid phosphatidylserine.

MATERIALS AND METHODS

Materials. Ins(1,4,5)P_3, Ins(1,4)P_2, Ins(1,2,3,4,5,6)P_6, and purine nucleoside phosphorylase were obtained from Sigma. Ins(1,3,4,5)P_4, *di*C8 PI(4)P, *di*C8 PI(5)P, *di*C8 PI(4,5)P_2, *di*C8 PI(3,4)P_2, and *di*C8 PI(3,4,5)P_3 were obtained from Echelon Biosciences Inc. Brain PI(4,5)P_2, brain L-α-phosphatidylserine, *di*C8 L-α-phosphatidylserine, and egg L-α-phosphatidylcholine were obtained from Avanti Polar Lipids Inc. 7-Methyl-6-thioguanosine (MESG) was obtained from Berry & Associates.

Expression and Purification of IPPRp. The gene for IPPRp[2] was located in a salivary gland cDNA library during the course of an EST sequencing project (*12*). The sequence included the coding region for a signal peptide. Using the N-terminal sequence (AKERDFTIHVATXNVNGRKPTTITNLIGQN) from a sample isolated from salivary gland homogenate (J. M. C. Ribeiro, unpublished data) as a guide, the cDNA was modified to remove the signal sequence and to insert an NdeI restriction site and an ATG initiation codon at the 5′-end of the modified gene. This sequence was cloned into the pET17b expression vector and moved into *Escherichia coli* strain BL21(DE3)pLys S for protein production. Cells were grown in LB medium at 37 °C, and the protein was produced as inclusion bodies using methods described previously (*13*). Inclusion bodies were dissolved in 6 M guanidine hydrochloride (pH 8.0) and reduced by adding DTT to a concentration of 10 mM. The protein was refolded by dilution into a large excess of 20 mM Tris-HCl (pH 8.0), 0.6 M NaCl, and 2.5 mM DTT. After stirring had been carried out overnight, the solution was centrifuged to remove precipitation. The folded material was concentrated in a tangential flow filtration device and purified by gel filtration chromatography on Sephacryl S-100 followed by cation exchange chromatography on SP-Sepharose.

Preparation of Phospholipid Vesicles. Long-chain phospholipids were dissolved in chloroform. After the appropriate mixture of stock solutions, the solvent was evaporated under a stream of nitrogen and the dried phospholipids were suspended in 20 mM Tris-HCl (pH 7.4), 1 mM $MgCl_2$, and 150 mM NaCl. Large unilamellar vesicles were formed by extrusion of this suspension through 100 nm pore diameter polycarbonate filters using a LiposoFast (Avestin) extrusion device.

Enzymatic Assays. Assays were performed using the continuous coupled inorganic phosphate detection system originally described by Webb (*14*) and used to assay IPP by Chi et al. (*15*) or with an end point ammonium molybdate-based assay described by Ribeiro et al. (*16*) and similar to that used by Chi et al. (*15*). In the coupled system, phosphate generated by the enzymatic reaction is used by purine nucleoside phosphorylase to cleave 7-methyl-6-thioguanosine (MESG) producing the purine base and ribose 1-phospate. The reaction was followed as an increase in absorbance at 360 nm. A molar extinction coefficient of 11 200 M^{-1} cm^{-1} has been determined for the change in absorbance due to phosphorolysis (*14*). Assays were performed in 0.8 mL volumes using 1 mL cuvettes maintained at 30 °C in a Varian Cary 100 spectrophotometer. The reaction buffer was 20 mM Tris-HCl (pH 7.4), 1 mM $MgCl_2$, and 150 mM NaCl. MESG was added to the reaction buffer to a concentration of 400 μM and purine nucleoside phosphorylase to a concentration of 0.175 mg/mL. Substrate was then added to concentrations of 5−500 μM, and after the equilibration of temperature, IPPRp was added at 2−18 nM depending on the experiment. Initial velocities were calculated from changes in absorbance during the first 0.1−2 min of the reaction. The first-order rate constant k_{obs} was calculated by fitting the reaction progress curves to the equation for a single-exponential increase to maximum.

The ammonium molybdate assay was run in 150 μL volumes using 20 mM Tris-HCl (pH 7.4), 150 mM NaCl, and 1 mM $MgCl_2$ as the reaction buffer. The reaction mixtures were incubated at 30 °C, and the reactions were stopped by adding the acid molybdate reagent; after development, the absorbance of each well was recorded at 650 nm. Phosphate production was assessed by comparison with a standard curve.

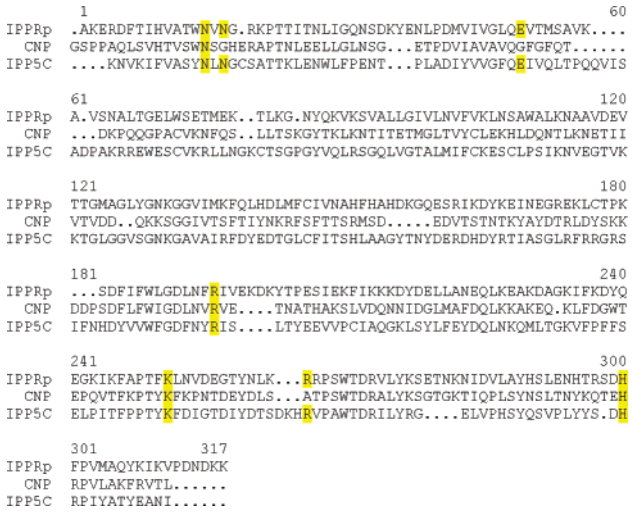

FIGURE 1: IPPRp amino acid sequence and comparison with members of the IPP family. Sequence alignment of the mature polypeptide of IPPRp with the salivary nitric oxide transport protein from *C. lectularis* (CNP) and the IPP5C domain from SPsynaptojanin. The conserved residues corresponding to those found to interact with the bound metal ion and bound Ins(1,4)P_2 in the SPsynaptojanin crystal structure are highlighted in yellow.

RESULTS

Cloning and Expression of IPPRp. The cDNA for IPPRp was identified in a database of expressed sequence tags obtained from a salivary gland cDNA library. The sequence encoded a 36.5 kDa protein similar to type II IPPs from a variety of organisms (Figure 1). Comparison with an experimentally determined N-terminal amino acid sequence from a sample of the protein isolated from salivary gland homogenates (J. M. C. Ribeiro, unpublished data) revealed

[2] The complete cDNA sequence of IPPRp has been deposited in GenBank with the accession number U70037.

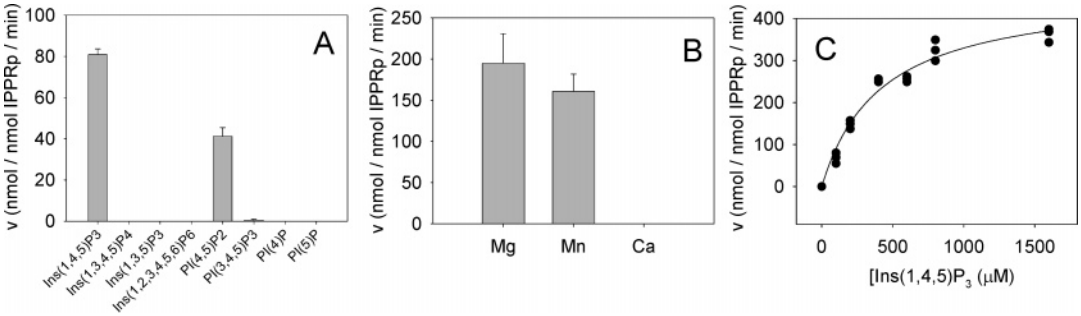

FIGURE 2: Enzymatic activities of IPPRp. (A) Screening of inositol phosphates and phosphoinositides as substrates for IPPRp using the continuous assay (mean ± standard error). Substrate concentrations were as follows: 50 μM Ins(1,4,5)P_3, 50 μM Ins(1,3,4,5)P_4, 50 μM Ins(1,3,5)P_3, 50 μM Ins(1,2,3,4,5,6)P_6, 7.5 μM PI(4,5)P_2 (C8), 7.5 μM PI(3,4,5)P_3 (C8), 7.5 μM PI(4)P (C8), and 100 μM PI(5)P (C8). The enzyme concentration was 18.75 nM. (B) Effect of divalent cations on catalytic rate. Assays were performed in the presence of 100 μM Ins(1,4,5)P_3 and either $MgCl_2$, $MnCl_2$, or $CaCl_2$ (each at 1 mM). The enzyme concentration was 18.75 nM. (C) Steady state kinetic analysis of hydrolysis of Ins(1,4,5)P_3 by IPPRp using the ammonium molybdate assay. Initial velocity data were fit to the Michaelis−Menten equation using nonlinear regression.

the presence of a 20-amino acid signal peptide, leaving a 34.4 kDa protein after cleavage and suggesting secretion of the protein into the saliva. The protein is most similar to the IPP5C catalytic domain of SPsynaptojanin (*11*) and the nitric oxide transport protein from the saliva of the bed bug *Cimex lectularis* (*17*, *18*; Figure 1). The latter is a member of the IPP family which has no enzymatic activity but binds a single heme molecule. There was no indication of heme or nitric oxide binding by the isolated IPPRp, suggesting that its function differed from that of the *C. lectularis* protein. Amino acid sequence alignments show that the IPPRp sequence corresponds quite precisely to the globular SPsynaptojanin catalytic domain whose structure has been determined (*11*; Figure 1). Unlike the *Cimex* protein, the structure of which has also been determined (*17*), IPPRp exhibited conservation of all amino acid residues implicated in metal and substrate binding in the SPsynaptojanin−Ins(1,4)P_2 complex, indicating that IPPRp was probably enzymatically active (Figure 1).

Reaction of IPPRp with Soluble Inositol Phosphates and Phosphoinositides. Recombinant IPPRp was tested against a variety of soluble inositol phosphates and phosphoinositides in reaction mixtures supplemented with divalent cations. Of the soluble inositols, only Ins(1,4,5)P_3 exhibited detectable product formation, while Ins(1,3,4,5)P_4, Ins(1,3,5)P_3, and Ins(1,2,3,4,5,6)P_6 (phytic acid) did not (Figure 2A). Apparently, phosphorylation at the D3 position of the inositol ring strongly inhibits either binding or catalysis.

The enzyme exhibited selectivity for certain divalent cations (Figure 2B). Both magnesium and manganese supported the reaction, but the enzyme was inactive in the presence of 1 mM calcium. Steady state kinetic parameters were calculated for Ins(1,4,5)P_3 hydrolysis by nonlinear fitting to the Michaelis−Menten equation, yielding a K_m value of 421 μM and a V_{max} of 468 nmol of product formed (nmol of IPPRp)$^{-1}$ min^{-1} (Figure 2C).

Phosphoinositides were also hydrolyzed by IPPRp. PI(4,5)P_2 was a far better substrate than PI(3,4,5)P_3, which supported little product formation (Figure 2A). PI(3,5)P_2, PI(4)P, and PI(5)P gave no detectable product, indicating that the phosphate at position D4 is necessary for removal of the D5 phosphate but is not itself hydrolyzed in the absence of a D5 phosphate. Thin-layer chromatography of the reaction product of brain PI(4,5)P_2 hydrolysis migrated with a standard of brain PI(4)P, a fact consistent with the specificity of IPPRp for 5-dephosphorylation (data not shown).

Allosteric Activation of PI(4,5)P_2 Hydrolysis by the Substrate. The kinetics of PI(4,5)P_2 hydrolysis were evaluated using substrate having C8 fatty acid chains. This short-chain substrate is monodisperse in aqueous buffers, thereby eliminating the effect of bulk surface binding to micelles or vesicles, and allowing analysis of reaction kinetics under solution conditions. Plots of initial velocity versus *di*C8 PI(4,5)P_2 concentration were clearly sigmoidal (Figure 3A), suggesting allosteric activation of IPPRp by the substrate. The reaction velocity data were subjected to a simple kinetic analysis by fitting to the Hill equation (eq 1):

$$v = V_{max}[S]^h/([S]^h + K_{0.5}{}^h) \quad (1)$$

where v is the initial velocity, h is the Hill coefficient, and $K_{0.5}$ is the substrate concentration at which v is half-maximal. Substrate binding was positively cooperative, with a Hill coefficient of 4.7, suggesting an activation mechanism involving binding at a minimum of four sites in addition to the catalytic site.

Allosteric Activation of Hydrolysis of PI(4,5)P_2 and PI(3,4,5)P_3 by PI(4)P. In the absence of activators, *di*C8 PI(3,4,5)P_3 was hydrolyzed much more slowly than *di*C8 PI(4,5)P_2. However, addition of *di*C8 PI(4)P, the product of hydrolysis of PI(4,5)P_2, to reaction mixtures containing *di*C8 PI(3,4,5)P_3 greatly increased the rate of phosphate production (Figure 4A). As expected, PI(4)P was not a substrate for IPPRp, as indicated by a lack of phosphate production when provided to the enzyme by itself (Figure 4B). Nevertheless, addition of PI(3,4,5)P_3 to a reaction mixture containing PI(4)P alone resulted in an increase in reaction rate comparable to that seen when PI(4)P was added to a reaction mixture containing only PI(3,4,5)P_3 (Figure 4A). These results indicated that the product, PI(4)P, can also activate IPPRp by an allosteric mechanism.

PI(4)P also stimulated the dephosphorylation of PI(4,5)P_2 by IPPRp. When *di*C8 PI(4)P was added to reaction mixtures at a fixed concentration of 70 μM, the plots of initial velocity versus *di*C8 PI(4,5)P_2 concentration changed from sigmoidal in the absence of activator to hyperbolic, with higher reaction rates at low substrate concentrations in the presence of PI(4)P than in its absence (Figure 3B). This result

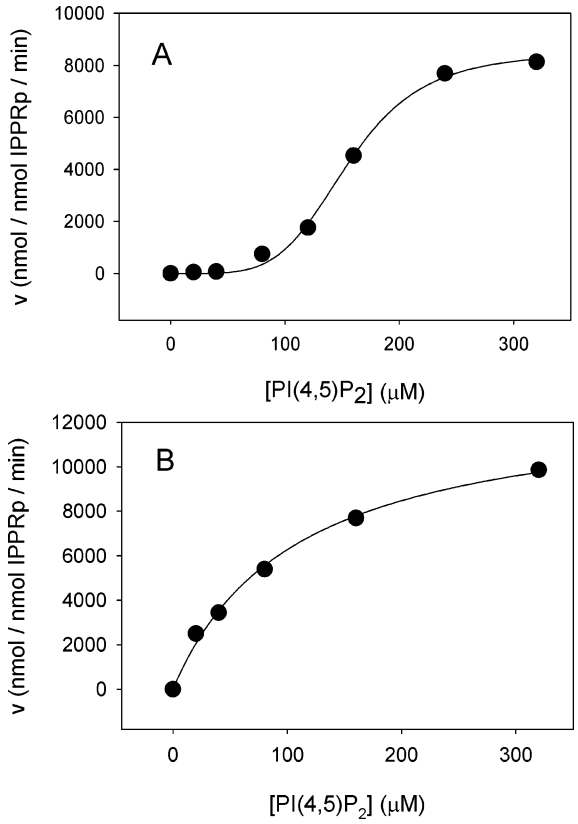

FIGURE 3: Hydrolysis of *di*C8 PI(4,5)P_2 by IPPRp. (A) Concentration dependence of PI(4,5)P_2 hydrolysis. Reactions were performed in a total volume of 400 μL and started by addition of 0.002 nmol of IPPRp. Initial velocities (●) were determined from progress curves, and the data were fitted to eq 1 (—). V_{max} = 8516 nmol of product (nmol of IPPRp)$^{-1}$ min^{-1}; $K_{0.5}$ = 156 μM, and h = 4.7. (B) Concentration dependence of PI(4,5)P_2 hydrolysis in the presence of 70 μM *di*C8 PI(4)P. Reactions were performed as described for panel A. Initial velocities (●) were determined from progress curves, and the data were fitted to the Michaelis−Menten equation (—). V_{max} = 13 037 nmol of product (nmol of IPPRP)$^{-1}$ min^{-1}, and the apparent K_m = 108 μM.

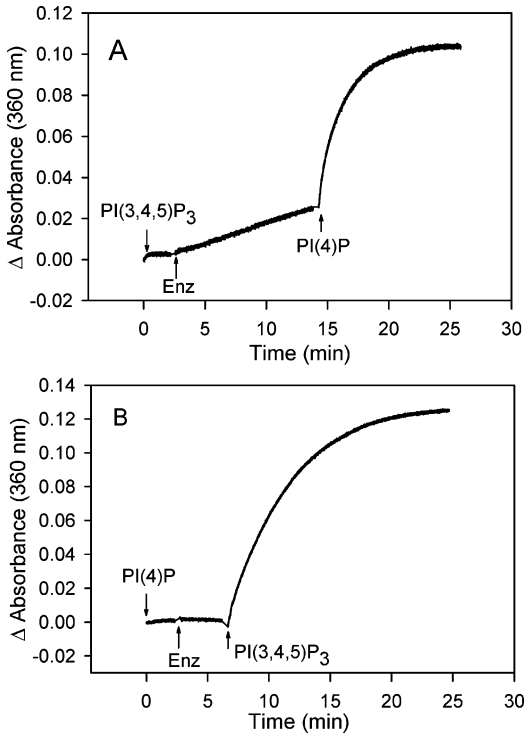

FIGURE 4: Reaction progress curves showing allosteric activation of hydrolysis of PI(3,4,5)P_3 by PI(4)P. Arrows are labeled to indicate the point at which components were added. (A) Progress curve showing addition of PI(4)P (20 μM) followed by IPPRp (Enz) and then PI(3,4,5)P_3 (12 μM). (B) Addition of PI(3,4,5)P_3 (12 μM) followed by IPPRp and then PI(4)P (20 μM). (C) PI(3,4,5)P_3 (12 μM) and PI(4)P (20 μM) added together, followed by IPPRp. The enzyme concentration in all cases was 18.75 nM.

is consistent with an activation mechanism involving noncatalytic allosteric sites which bind PI(4)P.

Kinetics of PI(4)P Activation. When the concentrations of *di*C8 PI(4,5)P_2 or *di*C8 PI(3,4,5)P_3 were held constant and the concentration of the nonsubstrate activator PI(4)P was varied, PI(4)P concentration-dependent rate increases were seen (Figure 5). Values for k_{obs}, the observed first-order rate constant for hydrolysis, were calculated, and the dependence of k_{obs} on PI(4)P concentration was determined. The relationship was sigmoidal for both substrates, and the data were analyzed with a variation of eq 1 (eq 2):

$$k_{obs} = k_{obs-max}[A]^h/([A]^h + K_{0.5}{}^h) + k_{obs-0} \qquad (2)$$

in which $k_{obs-max}$ is the maximal value for k_{obs} in the activated state, A is the activator, h is the Hill coefficient, $K_{0.5}$ is the activator concentration at one-half $k_{obs-max}$, and k_{obs-0} is the minimum k_{obs} value fit as a separate parameter. The fits produced values for the Hill coefficient of 2.6 for PI(4,5)P_2 and 3.1 for PI(3,4,5)P_3, indicating cooperative binding of at least three to four molecules of the allosteric inducer PI(4)P per molecule of IPPRp (Table 1). Full activation resulted in large increases in catalytic efficiency of 87- and 58-fold for hydrolysis of PI(4,5)P_2 and PI(3,4,5)P_3, respectively (Table 1).

Effect of PI(3,4)P_2 and Ins(1,4)P_2 on PI(4,5)P_2 Hydrolysis. To examine the specificity of the allosteric sites for specific headgroup structures and the importance of fatty acid chains in activation, PI(3,4)P_2 and Ins(1,4)P_2 were tested as activators of IPPRp. PI(3,4)P_2 was a weaker activator of hydrolysis of PI(4,5)P_2 by IPPRp than PI(4)P (Figure 5A). Ins(1,4)P_2, at a concentration of 100 μM, did not cause a detectable increase in the rate of PI(4,5)P_2 hydrolysis (data not shown).

Allosteric Activation of Hydrolysis of PI(4,5)P_2 and PI(3,4,5)P_3 by Soluble PS. The anionic phospholipid PS was tested for its effect on the activity of IPPRp. Again, short-chain (C8) derivatives of both PS and the substrates were used to create a monodisperse reaction mixture. Like *di*C8 PI(4)P, soluble *di*C8 PS stimulated hydrolysis of both substrates by IPPRp, producing a sigmoidal concentration dependence of k_{obs} at a fixed concentration of the substrates (Figure 6). The Hill coefficients again indicated positive cooperativity and binding of at least three to four molecules of inducer. The apparent affinity of IPPRp for soluble PS, as estimated by the $K_{0.5}$ values, is approximately 4-fold lower than for PI(4)P (Table 1). Like PI(4)P, PS stimulation resulted in large increases in catalytic efficiency of 113- and 33-fold for PI(4,5)P_2 and PI(3,4,5)P_3, respectively (Table 1).

Activation of PI(4,5)P_2 Hydrolysis by PS in a Vesicular System. The activity of IPPRp against vesicular substrates was evaluated using phospholipids with long-chain fatty acids. Both PS and PC were used as diluents to detect any specific stimulatory effects of PS. When PI(4,5)P_2 was

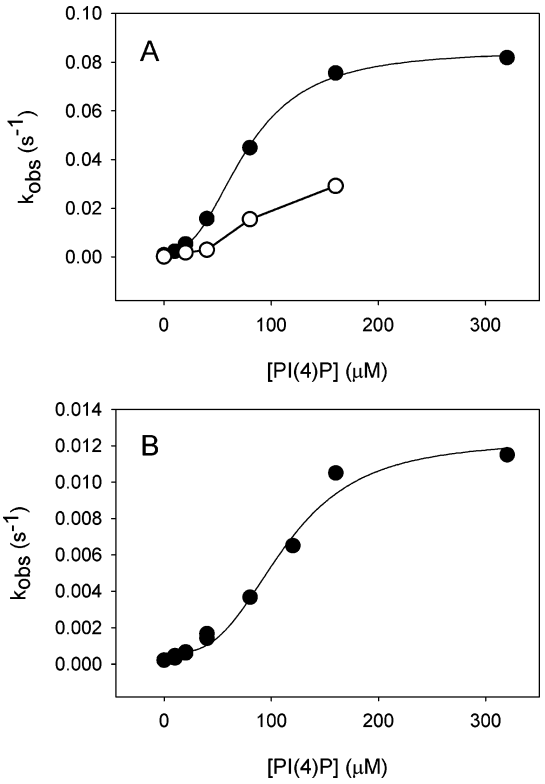

FIGURE 5: Concentration dependence of activation of IPPRp by *di*C8 PI(4)P and *di*C8 PI(3,4)P_2. (A) Concentration dependence of activation of hydrolysis of PI(4,5)P_2 by PI(4)P and PI(3,4)P_2. Observed first-order rate constants were calculated from reaction progress curves (●) at a fixed concentration of 20 μM PI(4,5)P_2. The data were fitted to eq 2 (—), and the resulting parameters are given in Table 1. The enzyme concentration was 6.25 nM. The ability of PI(3,4)P_2 to activate IPPRp was also tested (○). The assays were run in a manner identical to the manner of those with PI(4,5)P_2 except with a maximal concentration of 160 μM PI(3,4)P_2. (B) Concentration dependence of activation of hydrolysis of PI(3,4,5)P_3 by PI(4)P. Reactions were run as described for panel A [20 μM PI(3,4,5)P_3], except with an enzyme concentration of 18.75 nM. The data (●) were fitted to eq 2 (—), and the resulting parameters are given in Table 1.

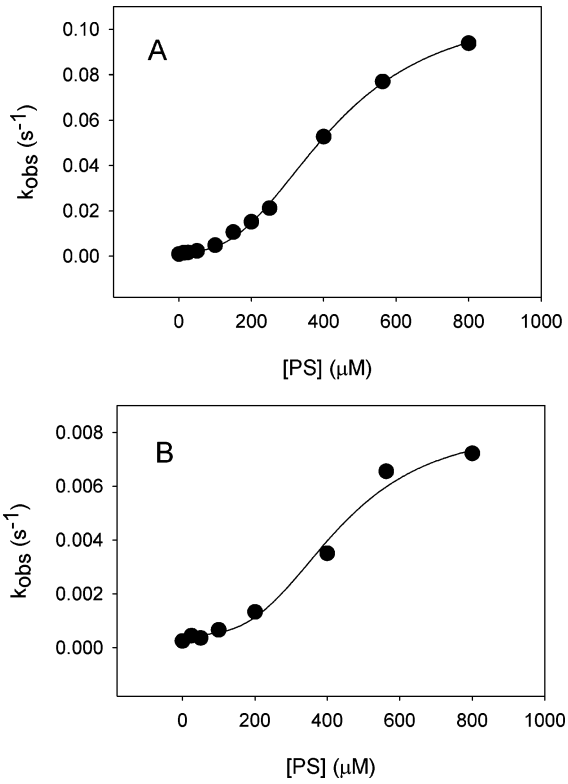

FIGURE 6: Concentration dependence of activation of IPPRp by *di*C8 PS. (A) Concentration dependence of activation of hydrolysis of PI(4,5)P_2 by PS. Observed first-order rate constants were calculated from reaction progress curves (●) at a fixed concentration of 20 μM PI(4,5)P_2. The data were fitted to eq 2 (—), and the resulting parameters are given in Table 1. The enzyme concentration was 6.25 nM. (B) Concentration dependence of activation of hydrolysis of PI(3,4,5)P_3 by PS. Reactions were run as described for panel A [20 μM PI(3,4,5)P_3], except with an enzyme concentration of 18.75 nM. The data (●) were fitted to eq 2 (—), and the resulting parameters are given in Table 1.

Table 1: Kinetic Parameters for Activation of *Di*C8 PI(4,5)P_2 and *Di*C8 PI(3,4,5)P_3 Hydrolysis by IPPRp in the Presence of Activators *Di*C8 PI(4)P and *Di*C8 PS Obtained by Fitting to eq 2

substrate	activator	$k_{obs-max}$[a]	h	$K_{0.5}$[b]	$(k_{cat}/K_m)_{min}$[c]	$(k_{cat}/K_m)_{max}$[d]
PI(4,5)P_2	PI(4)P	8.3	2.6	76	1.5×10^5	1.3×10^7
PI(3,4,5)P_3	PI(4)P	1.2	3.1	112	1.1×10^4	6.4×10^5
PI(4,5)P_2	PS	10.9	2.7	423	1.5×10^5	1.7×10^7
PI(3,4,5)P_3	PS	0.8	3.1	429	1.3×10^4	4.3×10^5

[a] In inverted seconds ($\times 10^2$). [b] In micromolar. [c] Observed value for k_{cat}/K_m in the absence of activator (M^{-1} s^{-1}). [d] Calculated value for the maximum value of k_{cat}/K_m from fitting to eq 2 (M^{-1} s^{-1}).

incorporated into PS vesicles, product formation was dramatically stimulated in comparison to that in identically prepared PC-containing vesicles (Figure 7). Unlike the reaction rates with *di*C8 phospholipids, the reaction rates at fixed concentrations of PI(4,5)P_2 in PS vesicles decreased with a decrease in the mole fraction of substrate, indicating that an interfacial model for catalysis could be applied (*19*, *20*; Figure 7A,B). In this model, bound enzyme diffuses in two dimensions over the lipid surface, hydrolyzing substrate molecules it encounters in its path. The reaction is described by eq 3

$$E + A \underset{k_{-1}}{\overset{k_1}{\rightleftharpoons}} EA \quad EA + B \underset{k_{-2}}{\overset{k_2}{\rightleftharpoons}} EAB \underset{k_{-3}}{\overset{k_3}{\rightleftharpoons}} EA + Q \quad (3)$$

where A is the bulk phospholipid vesicle surface, B is the phospholipid substrate incorporated into the bulk surface, and Q is the reaction product.

Surface-dilution kinetic methods (*20*) were used to analyze the dependence of enzyme activity on bulk substrate concentration and mole fraction of substrate in phospholipid vesicles (Figure 7A). Kinetic parameters were determined using eq 4 (*20*)

$$v = V_{max}(A)(B)/[K_s^A K_m^B + K_m^B(A) + (A)(B)] \quad (4)$$

where (A) is the total concentration of phospholipid including diluent and substrate, (B) is the mole fraction of substrate phospholipid contained in the bulk phase, K_s^A is equal to k_{-1}/k_1, and K_m^B is equal to $(k_{-2} + k_3)/k_2$. The data showed IPPRp to be a highly efficient interfacial enzyme for PI(4,5)P_2 hydrolysis in the context of PS vesicles (Table 2).

Product formation rates with PC vesicles containing PI(4,5)P_2 were far lower than those with PS vesicles (Figure 7C). Unlike PS, PC exhibited no stimulating effect and appeared to act simply as a diluent. At 0.05 mole fraction of PI(4,5)P_2 and a concentration of 40 μM, the reaction rate

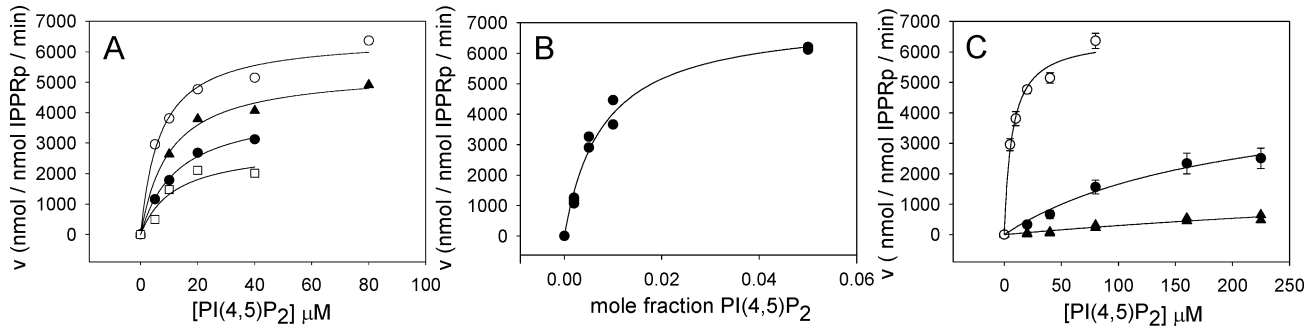

FIGURE 7: Hydrolysis of PI(4,5)P_2 by IPPRp in mixed phospholipid vesicles. (A) Initial velocities measured using the coupled assay as a function of PI(4,5)P_2 concentration measured at different mole fractions in PS vesicles: (○) 0.05, (▲) 0.01, (●) 0.005, and (□) 0.002 mole fraction. The experiments were performed under the conditions described in Materials and Methods using an enzyme concentration of 2 nM. (B) Initial velocities for hydrolysis of PI(4,5)P_2 (40 μM) as a function of mole fraction in PS vesicles under standard conditions with an enzyme concentration of 2 nM. The data were fitted to a rectangular hyperbola from which a value for V_{max} could be determined. (C) Comparison of enzymatic activity of IPPRp toward PI(4,5)P_2 in different phospholipid environments: (○) 0.05 mole fraction in PS, (●) 0.05 mole fraction in 3:1 PC/PS vesicles, and (▲) 0.05 mole fraction in PC vesicles. The enzyme concentration was 2 nM.

Table 2: Surface Dilution Kinetic Parameters (±standard error) for the Reaction of IPPRp Hydrolysis of PI(4,5)P_2 in PS Large Unilamellar Vesicles

V_{max}[a]	7185 ± 353
K_s^{A}[b]	7.9 ± 1.14
K_m^{B}[c]	0.0035 ± 0.0002
k_{cat}/K_m^{B}[d]	2×10^6

[a] Nanomoles of product per nanomole of enzyme per minute. [b] Millimolar, surface binding model. [c] Mole fraction. [d] Mole fraction^{-1} min^{-1}.

for PC vesicles was approximately 80-fold lower than for PS vesicles under the same conditions (Figure 7C). In mixed vesicles containing a 3:1 PC:PS ratio and 0.05 mole fraction PI(4,5)P_2, reaction rates were intermediate between those obtained with homogeneous PS and PC, indicating a quantitative relationship between simulation and the fraction of PS contained in vesicles (Figure 7C).

DISCUSSION

The secreted enzyme IPPRp is a typical type II IPP that hydrolyzes phosphoinositides at higher rates than soluble inositol phosphates. IPPRp is selective for PI(4,5)P_2, the phospholipid precursor of the signaling molecule Ins(1,4,5)-P_3, and itself an important regulator of membrane trafficking and cytoskeletal reorganization. Substrates having a D3 phosphate are hydrolyzed at lower rates than those lacking phosphate at this position, while substrates lacking a phosphate at the D4 position yield no detectable product. IPPRp is activated at membrane interfaces, specifically those containing anionic phospholipids. These facts suggest that IPPRp acts physiologically to regulate the bulk level of membrane phosphoinositide available for signaling pathways and other cellular processes.

Unexpectedly, we found strong stimulation of phosphoinositide hydrolysis by the soluble *di*C8 forms of PI(4,5)P_2, PI(4)P, and PS, suggesting allosteric activation by anionic phospholipids. Since the nonsubstrate molecules PI(4)P and PS also activate IPPRp in a manner similar to that of the substrate PI(4,5)P_2, the allosteric sites are apparently noncatalytic. This behavior is similar to that reported for the PI-specific phospholipase C in its reaction with fluorescent substrate analogues, where a second molecule of substrate binds to a noncatalytic site and stimulates activity of the monomeric enzyme (*21*).

Binding of *di*C8 PI(4,5)P_2, PI(4)P, and PS with IPPRp is cooperative, and analyses of kinetic data by the Hill equation indicated the presence of three to four allosteric sites. The involvement of multiple sites suggests a mechanism whereby phospholipid molecules are ordered on the membrane interaction surface of the protein, perhaps causing a conformational change in the enzyme, or otherwise facilitating substrate binding. In the natural system, where IPPRp binds to the surfaces of cells (or platelets), anionic phospholipids would activate the enzyme, and the degree of activation would depend on the mole fraction of activators contained in the membrane. If anionic phospholipids were present at sufficient density to occupy all allosteric sites, an increase in the catalytic efficiency of 30−100-fold for PI(4,5)P_2 and PI(3,4,5)P_3 over that of the unactivated enzyme would be expected, on the basis of the in vitro results.

The sigmoidal kinetics of activation of IPPRp by *di*C8 phospholipids are apparently not due to the formation of micelles or aggregates prior to binding. The concentrations of *di*C8 phospholipids used here are far below their reported CMC values. *Di*C8 PS has a reported CMC of 2.28 mM (*22*), and the *di*C8 phosphoinositides are considered to be completely soluble at concentrations of <5 mM (Echelon Research Laboratories, technical note). If substrate and activator were forming mixed micelles during the reaction, a surface dilution effect would be expected. We found here that mixtures of soluble *di*C8 PI(4,5)P_2 and soluble *di*C8 PS produced the opposite effect. The reaction rates with short-chain soluble phospholipids increased as the mole fraction of substrate was reduced. Conversely, when long-chain PI-(4,5)P_2/PS mixed vesicles were used as a substrate, surface dilution kinetics were observed in which reaction rates decreased with a decrease in the mole fraction of substrate. This behavior is characteristic of an interfacial system and strongly supports the idea that short-chain substrates and activators are bound directly from solution.

The allosteric sites of IPPRp show some selectivity for particular anionic headgroup structures, and the presence of a diacylglycerol moiety in an activator molecule is essential. PI(3,4)P_2 is a less potent activator than PI(4)P, suggesting that a phosphate group at the D3 position acts to reduce the

binding affinity. The diacylglycerol requirement is indicated by the complete lack of activity of Ins(1,4)P_2, the product of Ins(1,4,5)P_3 hydrolysis. Nevertheless, the similarities between PS activation and activation by PI(4,5)P_2 and PI(4)P suggest that these compounds may bind at the same sites and that the allosteric sites recognize a relatively diverse array of anionic headgroups.

Activation by products of phosphate hydrolysis has also been seen with PTEN, a structurally unrelated phosphoinositide phosphatase which removes phosphate from the D3 position (*23*, *24*). In that system, PI(4,5)P_2 is the activating molecule, while the substrate itself does not appear to activate. In the absence of activator, PTEN hydrolyzes PI(3,4,5)P_3 at a considerably higher rate than PI(3,4)P_2. Addition of PI(4,5)P_2 dramatically increases the hydrolysis rate of PI(3,4)P_2 but only modestly increases the rate of PI(3,4,5)P_3 cleavage (*23*, *24*). Site-directed mutagenesis experiments with PTEN indicated that a putative phosphoinositide recognition motif near the N-terminus of the catalytic domain serves as the allosteric binding site (*24*, *25*). The locations of the allosteric sites in IPPRp are not presently known but are likely to lie on the face of the enzyme that contacts the membrane surface, since PS, PI(4)P, and substrate would normally be found as components of the same membrane surface. We also do not know if allosteric activation of this type is a general feature of type II IPPs. If so, this mechanism of regulation could play a role in many cellular processes and may provide clues about how the phosphoinositide composition in membranes is regulated.

IPPRp occurs in the saliva of *R. prolixus* where it is injected into the host during blood feeding (*26*). On the basis of its enzymatic function, it apparently acts to reduce the bulk concentration of PI(4,5)P_2 and PI(3,4,5)P_3 in the plasma membrane of cells or platelets. Changes in the concentration of these phospholipids would have many potential effects, including the elimination of substrates for phospholipase C and PI3-kinase, changes in cytoskeletal architecture, and changes in membrane trafficking and vesicle secretion.

The phospholipid composition of the plasma membrane is normally asymmetrical with anionic phospholipids being sequestered in the inner leaflet (*27*, *28*). Also, the known activities of IPPs are all intracellular processes. How would an extracellular enzyme interact with phospholipid forms occurring only in the inner leaflet? Perhaps the rapid and dramatic loss of asymmetry [phospholipid scrambling (*27*)] that occurs on activation of platelets (and other cell types such as mast cells following degranulation) would allow access of IPPRp to its substrate and activators. Phospholipid scrambling results in the exposure of phosphatidylserine and presumably phosphoinositides, on the surface of platelets, and this exposure would act to stimulate IPPRp. The relatively rapid and nonspecific equilibration of phospholipid composition between the inner and outer leaflets (*29*) may allow IPPRp to reduce the overall levels of 5-phosphorylated phosphoinositides in the membrane by hydrolyzing them in the outer leaflet.

ACKNOWLEDGMENT

We thank Rosanne Hearn and My Van Pham for technical assistance, Drs. Don Champagne, Ben Mans, and Ivo Francischetti for discussion of the results, and Drs. Thomas Wellems and Robert Gwadz for general support of the project.

REFERENCES

1. Erneux, C., Govaerts, C., Communi, D., and Pesesse, X. (1998) The diversity and possible functions of the inositol polyphosphate 5-phosphatases, *Biochim. Biophys. Acta 1436*, 185−199.
2. Mitchell, C. A., Gurung, R., Kong, A. M., Dyson, J. M., Tan, A., and Ooms, L. M. (2002) Inositol polyphosphate 5-phosphatases: Lipid phosphatases with flair, *IUBMB Life 53*, 25−36.
3. Whisstock, J. C., Wiradjaja, F., Waters, J. E., and Gurung, R. (2002) The structure and function of catalytic domains within inositol polyphosphate 5-phosphatases, *IUBMB Life 53*, 15−23.
4. Guo, S., Stolz, L. E., Lemrow, S. M., and York, J. D. (1999) SAC1-like domains of yeast SAC1, INP52, and INP53 and of human synaptojanin encode polyphosphoinositide phosphatases, *J. Biol. Chem. 274*, 12990−12995.
5. Simonsen, A., Wurmser, A. E., Emr, S. D., and Stenmark, H. (2001) The role of phosphoinositides in membrane transport, *Curr. Opin. Cell Biol. 13*, 485−492.
6. Gillooly, D. J., Simonsen, A., and Stenmark, H. (2001) Cellular functions of phosphatidylinositol 3-phosphate and FYVE domain proteins, *Biochem. J. 355*, 249−258.
7. Tsujishita, Y. (2003) Structural genomics of lipid signaling domains, *Oncol. Res. 13*, 421−428.
8. Berridge, M. J., and Irvine, R. F. (1989) Inositol phosphates and cell signalling, *Nature 341*, 197−205.
9. Majerus, P. W., Kisseleva, M. V., and Norris, F. A. (1999) The role of phosphatases in inositol signaling reactions, *J. Biol. Chem. 274*, 10669−10672.
10. Kisseleva, M. V., Wilson, M. P., and Majerus, P. W. (2000) The isolation and characterization of a cDNA encoding phospholipid-specific inositol polyphosphate 5-phosphatase, *J. Biol. Chem. 275*, 20110−20116.
11. Tsujishita, Y., Guo, S., Stolz, L. E., York, J. D., and Hurley, J. H. (2001) Specificity determinants in phosphoinositide dephosphorylation: Crystal structure of an archetypal inositol polyphosphate 5-phosphatase, *Cell 105*, 379−389.
12. Ribeiro, J. M. C., Andersen, J., Silva-Neto, M. A. C., Pham, V. M., Garfield, M. K., and Valenzuela, J. G. (2004) Exploring the sialome of the blood-sucking bug *Rhodnius prolixus*, *Insect Biochem. Mol. Biol. 34*, 61−79.
13. Andersen, J. F., Francischetti, I. M. B., Valenzuela, J. G., Schuck, P., and Ribeiro, J. M. C. (2003) Inhibition of hemostasis by a high affinity biogenic amine-binding protein from the saliva of a blood-feeding insect, *J. Biol. Chem. 278*, 4611−4617.
14. Webb, M. R. (1992) A continuous spectrophotometric assay for inorganic phosphate and for measuring phosphate release kinetics in biological systems, *Proc. Natl. Acad. Sci. U.S.A. 89*, 4884−4887.
15. Chi, Y., Zhou, B., Wang, W. Q., Chung, S. K., Kwon, Y. U., Ahn, Y. H., Chang, Y. T., Tsujishita, Y., Hurley, J. H., and Zhang, Z. Y. (2004) Comparative mechanistic and substrate specificity study of inositol polyphosphate 5-phosphatase *Schizosaccharomyces pombe* Synaptojanin and SHIP2, *J. Biol. Chem. 279*, 44987−44995.
16. Ribeiro, J. M., Sarkis, J. J., Rossignol, P. A., and Spielman, A. (1984) Salivary apyrase of *Aedes aegypti*: Characterization and secretory fate, *Comp. Biochem. Physiol., Part B: Biochem. Mol. Biol. 79*, 81−86.
17. Weichsel, A., Maes, E. M., Andersen, J. F., Valenzuela, J. G., Shokhireva, T., Walker, F. A., and Montfort, W. R. (2005) Heme-assisted S-nitrosation of a proximal thiolate in a nitric oxide transport protein, *Proc. Natl. Acad. Sci. U.S.A. 102*, 594−599.
18. Valenzuela, J. G., and Ribeiro, J. M. C. (1998) Purification and cloning of the salivary nitrophorin from the hemipteran *Cimex lectularius*, *J. Exp. Biol. 201*, 2659−2664.
19. Berg, O. G., Gelb, M. H., Tsai, M. D., and Jain, M. K. (2001) Interfacial enzymology: The secreted phospholipase A_2-paradigm, *Chem. Rev. 101*, 2613−2654.
20. Carman, G. M., Deems, R. A., and Dennis, E. A. (1995) Lipid signaling enzymes and surface dilution kinetics, *J. Biol. Chem. 270*, 18711−18714.
21. Birrell, G. B., Zaikova, T. O., Rukavishnikov, A. V., Keana, J. F., and Griffith, O. H. (2003) Allosteric interactions within subsites of a monomeric enzyme: kinetics of fluorogenic substrates of PI-specific phospholipase C, *Biophys. J. 84*, 3264−3275.

22. Kleinschmidt, J. H., and Tamm, L. K. (2002) Structural transitions in short-chain lipid assemblies studied by ^{31}P NMR spectroscopy, *Biophys. J. 83*, 994−1003.
23. McConnachie, G., Pass, I., Walker, S. M., and Downes, C. P. (2003) Interfacial kinetic analysis of the tumour suppressor phosphatase, PTEN: Evidence for activation by anionic phospholipids, *Biochem. J. 371*, 947−955.
24. Campbell, R. B., Liu, F., and Ross, A. H. (2003) Allosteric activation of PTEN phosphatase by phosphatidylinositol 4,5-bisphosphate, *J. Biol. Chem. 278*, 33617−33620.
25. Lee, J. O., Yang, H., Georgescu, M. M., Di Cristofano, A., Maehama, T., Shi, Y., Dixon, J. E., Pandolfi, P., and Pavletich, N. P. (1999) Crystal structure of the PTEN tumor suppressor: Implications for its phosphoinositide phosphatase activity and membrane association, *Cell 99*, 323−334.
26. Ribeiro, J. M. C., Schneider, M., Jurberg, I. T., Galvao, J., and Guimaraes, J. A. (1998) Role of salivary antihemostatic components in blood feeding by triatomine bugs (Heteroptera), *J. Med. Entomol. 35*, 599−610.
27. Sims, P. J., and Wiedmer, T. (2001) Unraveling the mysteries of phospholipid scrambling, *Thromb. Haemostasis 86*, 266−275.
28. Heemskerk, J. W., Bevers, E. M., and Lindhout, T. (2002) Platelet activation and blood coagulation, *Thromb. Haemostasis 88*, 186−193.
29. Williamson, P., Bevers, E. M., Smeets, E. F., Comfurius, P., Schlegel, R. A., and Zwaal, R. F. (1995) Continuous analysis of the mechanism of activated transbilayer lipid movement in platelets, *Biochemistry 34*, 10448−10455.

BI052444J